DR. HEIDA L. DIEFENDERFER (Orcid ID : 0000-0001-6153-4565)

Article type : Articles

Storm-Driven Particulate Organic Matter Flux Connects a Tidal Tributary Floodplain Wetland, Main Stem River, and Estuary

Ronald M. Thom,[1] Stephen A. Breithaupt,[1] Heida L. Diefenderfer,[1] Amy B. Borde,[1] G. Curtis Roegner,[2] Gary E. Johnson,[1] and Dana L. Woodruff[1]

[1]Pacific Northwest National Laboratory, Marine Sciences Laboratory, 1529 West Sequim Bay Road, Sequim, Washington 98382 USA

[2]National Oceanic and Atmospheric Administration, National Marine Fisheries Service, Point Adams Field Station, 520 Heceta Place, Hammond, Oregon 97121 USA

Corresponding Author: H. Diefenderfer

heida.diefenderfer@pnnl.gov

Abstract

The transport of terrestrial plant matter into coastal waters is important to regional and global biogeochemical cycles, and methods for assessing and predicting fluxes in such dynamic environments are needed. We investigated the hypothesis that upon reconnection of a floodplain wetland to its main stem river, organic matter produced in the wetland would reach other parts of the ecosystem. If so, we can infer that the organic matter would ultimately become a source for the food web in the main stem river and estuary. To accomplish this, we adapted numerical hydrodynamic and transport modeling methods to estimate the mass of particulate organic matter (POM) derived from the annually senescent above-ground parts of herbaceous marsh plants (H-POM). The Finite-Volume Community Ocean Model (FVCOM), parameterized with flow, tide,

and above-ground biomass data, simulated H-POM mobilization from fluid shear stress during tidal exchange, flooding, and variable river flow; entrainment into the water column; transport via channel and overland flow; and entrapment when wetted surfaces dry. We examined export from a recently reconnected, restoring tidal emergent marsh on the Grays River, a tributary to the Columbia River estuary. Modeling indicated that hydrologically reconnecting 65 ha at the site resulted in export of about 96×10^3 kg of H-POM, primarily during pulsed storm flooding events in autumn and early winter. This exported mass amounted to about 19% of the summer peak above-ground biomass measured at the site. Of that 19%, about 48% (47×10^3 kg) was deposited downstream in the Grays River and floodplain wetlands, and the remaining 52% (50×10^3 kg) passed the confluence of the Grays River and the main stem estuary located about 7 km from the study site. The colonization of the restoring study site largely by non-native *Phalaris arundinacea* (reed canarygrass) may have resulted in 18–28% lower H-POM mobilization than typical marsh plant communities on this floodplain, based on estimates from regional studies of marshes dominated by less recalcitrant species. We concluded that restored floodplain wetlands can contribute significant amounts of organic matter to the estuarine ecosystem, and thereby contribute to the restoration of historical trophic structure.

Key words: allochthonous organic matter flux; dike breach; H-POM; hydrodynamic and transport modeling; lateral connectivity; marsh detritus; particulate organic matter; restoration; riparian zone; spatial subsidy; terrestrial-aquatic interface; tidal freshwater

Introduction

Studies since at least the 1950s have clearly demonstrated that particulate organic matter (POM) produced in wetlands of all kinds is exported to other parts of ecosystems where it can contribute to the detritus-based food web (e.g., Odum 1956; Teal 1962; Childers et al. 2000). Dissolved organic matter transported from wetlands along with benthic and planktonic algae can also be major contributors to the organic matter pool in estuaries (Haines 1977; Correll 1978; Odum 1984). The release of organic matter is often not steady. Rather, export occurs in pulses mediated by biological periodicity (e.g., productivity) and physical drivers such as floods, storms, or periods of high tidal amplitude (Junk et al. 1989; Odum et al. 1995; Mannino and Harvey 2000). Organic matter produced in terrestrial and aquatic ecosystems can be transported

to near-coastal systems through a process commonly referred to as "outwelling" (e.g., Nixon 1980; Dame et al. 1986; Wheatcroft et al. 2010). Outwelling is generally considered an important link in global geochemical cycles (Hope et al. 1997).

In our study area on the U.S. Pacific Northwest (PNW) coast, the tidal wetlands, seagrass meadows, and benthic algae exhibit high production rates (Thom 1984; Small et al. 1990; Emmett et al. 2000). Organic matter produced in PNW estuaries and river floodplains reaches the coastal water where it contributes to the coastal food web (Dahm et al. 1981; Small and Prahl 2004; Walsh et al. 2008). Further, planktonic larval exchange between estuaries and coastal waters is common (Johnson and Gonor 1982; Roegner 2000; Roegner et al. 2011). A growing body of information is demonstrating that this organic matter contributes significantly to fisheries resources important to the economies of the region, such as the iconic salmonids (Healy 1979; Sibert 1979; Simenstad and Wissmar 1985, Maier and Simenstad 2009).

Globally, approximately 25–50% of vegetated coastal habitats responsible for organic matter production and export to the nearshore ocean has been lost in the past 50 years (Duarte et al. 2013b). Presumably, historical levels of total primary production and total POM export have been correspondingly curtailed. Land conversion and development, including the construction of dikes and levees, have been the most pervasive human-linked alteration of floodplain and estuarine wetland habitats (Mitsch and Gosselink 2007). In the Columbia River estuary (defined as the 235 km tidal reach from Bonneville Dam to the Pacific Ocean), tidal forested, herbaceous, and shrub-scrub wetlands have been reduced by 20,734 ha (68-70%) since the late 1800s through agricultural development (i.e., forest removal, diking, farming, grazing) and urbanization (Marcoe and Pilson 2017). Eliminating or severely restricting hydrological connection between wetlands and surrounding ecosystems results in alterations to the flows of energy, materials and species between wetlands and the aquatic and riparian portion of the ecosystem (Naiman and Décamps 1997; Odum et al. 1995). Further, this "disintegration" of elements composing ecosystems restricts the ecosystem processes and services provided by the wetlands, such as groundwater recharge and sediment trapping. Efforts to restore and enhance coastal wetland ecosystems by breaching levees, removing dikes and levees, and retrofitting culverts are becoming increasingly common and successful in at least partially restoring many ecological functions and services (Simenstad and Thom 1996; Zedler 2001; Irving et al. 2011). Yet

managing and maximizing the benefits of wetland restoration requires quantifying and predicting the connections between wetlands and the wider hydrological system.

In the Columbia River estuary, POM historically formed the base of the food web, in contrast to present conditions in which fluvial phytoplankton appears to be predominant (Sherwood et al. 1990; Small et al. 1990). Sources of POM and phytoplankton include autochthonous generation within the estuary, allochthonous input from the Columbia River and the tributaries upstream of the estuary, and imports from the Pacific Ocean via tidal exchange (Roegner et al. 2011). Sherwood et al. (1990) concluded that the loss of marshes and swamps resulted in a comprehensive shift in the amount and quality of organic matter delivered to the food web in the lower river and estuary; i.e., an ~82% decline in the marsh macrodetritus mass reaching the estuary food web compared to the mass contributed historically. This is thought to have resulted in a shift of the food web base for juvenile salmon and other estuarine-dependent species from wetland-produced insects and epibenthic invertebrate prey to planktonic prey fed by water column primary producers in reservoirs above dams. Recent research employing stable isotope analysis of organic matter sources and fish tissues has shown that fluvial phytoplankton, vascular plants, and benthic diatoms, respectively, contributed 40, 46, and 14% of the organic matter of the diet of juvenile salmon feeding on invertebrate prey in the Columbia River estuary (Maier and Simenstad 2009; Maier et al. 2011). This information was an important driver of our research, because of the potential functional support afforded to threatened and endangered salmonids by restored floodplain habitats.

Our study was part of a comprehensive research effort supporting the Columbia Estuary Ecosystem Restoration Program, which is aimed at restoring ecosystems in the Columbia River estuary (Ebberts et al. 2017). Researchers measured the responses of tidal wetlands to tidal hydrological reconnection, and developed and implemented methods for predicting the effects of multiple restoration projects on the ecosystem (Diefenderfer et al. 2012; Ke et al. 2013; Diefenderfer et al. 2016). “Material flux” was recommended as an indicator of the ecosystem processes and realized functions among several response indicators that were assessed (Roegner et al. 2009). Specifically, our study addressed the following question: Does restoring hydrological connection facilitate the export of quantities of endogenously produced POM that could fuel the food web of the broader ecosystem? Using the framework described by Diefenderfer et al. (2011, 2016), we hypothesized that restoring hydrological interconnection

would allow for material exchange process and we investigated how much material would leave the system and whether that material could reach the broader estuary from sites located in tidal freshwater portions of tributary streams and rivers.

To address how the restoration of floodplain wetlands can affect the contribution of marsh macrophyte organic matter from production site to the broader ecosystem, we assessed the mass of vascular plant organic matter produced that is exported out of a tidal wetland after hydrological reconnection to the estuary. For this purpose, we focused on POM derived from the annually senescent above-ground parts of herbaceous marsh plants (H-POM). Our objective was to develop quantifiable information based on field data and modeling about how restoring the hydrological connectivity and the associated shift in plant communities of floodplain wetlands would affect the flow of energy as organic matter between wetlands and the broader ecosystem, recognizing that H-POM is only one component of organic matter flux. To that end, we first simulated the hydrologic and hydraulic characteristics that affect H-POM transport from a wetland, and then used mass-transport tracking simulation to estimate H-POM transport between the wetland source, the tributary floodplain, and ultimately the main stem of the Columbia River estuary.

Study Area and Site

Our study area was a tidal portion of the rainfall-dominated Grays River watershed, a major tributary to the main stem Columbia River (Fig. 1a). The study site, Kandoll Farm (KF site), is ~7 km upstream from the confluence of the Grays and Columbia Rivers. The confluence, at Grays Bay, is within the energy minimum reach (i.e., where the turbidity maximum normally occurs) of the Columbia River estuary system zone between river kilometers 21 and 39 (Jay et al. 2016). The 65 ha KF site was disconnected from Grays River and its floodplain by dikes along the river and across the floodplain, forming a parcel isolated from all but the most extreme annual flood events (Fig. 1). Beginning in the 1800s, logging of *Picea sitchensis* (Sitka spruce) forest and dike construction converted the landscape from a natural tidal freshwater spruce wetland to pastureland grazed by cattle. Water was only allowed to drain from the site through a small (~0.75 m diameter) top-hinged tide gate into Seal Slough. The tide gate essentially prevented water from flowing into the site at all surface-water levels except for those related to

flood events. During annual maximum flood events, water would flow into the site by overtopping the levee primarily along the main channel of the Grays River.

In 2005, hydrological reconnection to the KF site was undertaken by replacing the tide gate to Seal Slough with two ~4 m diameter culverts and by several small breaches along the main stem of Grays River. The new culverts restored water-level variations within the site that matched the timing and amplitude within unrestricted areas in Seal Slough, although floodwaters still overtop the remaining levees (Breithaupt and Khangaonkar 2008). Between 2005 and 2010, vegetation shifted from wet pasture grasses, *Trifolium pratense, T. repens, T. dubium* (clovers), and *Ranunculus repens* (creeping buttercup) to a mix of tidal freshwater emergent marsh species dominated by *Phalaris arundinacea* (reed canarygrass). These changes indicated that physical and biological processes were driving tidal wetland development.

Methods

Our period of analysis covers the seasonal changes from June 2006 through February 2007, i.e., post-restoration years one to two after culvert installation in 2005. We chose this seasonal time period because sampling showed that it represents the period of development of the maximum emergent wetland vegetation above-ground biomass density (i.e., dry weight per unit area) and the subsequent loss of biomass from floodplain wetlands during the winter (Small et al. 1990). In the PNW, the typical period of coastal wetlands flooding is during the late fall and early winter. Based on our field observations at the KF site and two other wetland sites over the period of 2004–2012, the majority of H-POM exchange between the site of production and offsite areas (Fig. 1b) appeared to occur as a flood pulse of material during these seasons.

Hydrodynamic Modeling

We employed deterministic results from a previously developed hydrodynamic model of the Grays River to evaluate the effect of hydraulic reconnection at restoration sites on the flooding of adjacent areas (Breithaupt and Khangaonkar 2008; Breithaupt and Lee 2011). The model domain included Grays River, Seal Slough, and the floodplain from the mouth of Grays River to approximately 8 km upstream (Fig. 2). The modeling geometry was based on high-resolution light detection and ranging topography data for the Grays River floodplain (Breithaupt and Khangaonkar 2008), field-surveyed cross sections of the Grays River and Seal Slough channels

(Diefenderfer et al. 2008), and hourly measurements of Grays River flow. Here, we further develop this model to assess the fate of H-POM derived at the KF site to the model domain through key processes: POM mobilization from fluid shear stress during tidal exchange, flooding, and variable river flow; entrainment in the water column; transport via channel and overland flow; and entrapment when wetted surfaces dry. The model was calibrated with field measurements of key water and vegetation variables (Appendix S1).

We used the hydrodynamic model Finite-Volume Community Ocean Model (FVCOM) (Chen et al. 2006) to simulate flow in Grays River including Seal Slough and Grays Bay. FVCOM is a three-dimensional finite-volume model that uses an unstructured grid (composed of triangular elements) for defining the system's complex geometry (Fig. 2). The hydrodynamic model solves depths, velocities, and water-surface elevations (WSEs) within the model domain based on the geometry of the system and the boundary conditions specified in the analysis. The model includes wetting and drying to control the inundation of land surfaces due to WSE changes from tidal and runoff forcing. FVCOM calculates friction losses at the bed-water interface via turbulent shear stress equations. These internal calculations of shear stress are critical to the simulation of the mobilization of H-POM from the study site, and are outlined in detail by Chen et al. (2006).

River flow and tidal inundation of wetlands directly affect mobilization and transport of H-POM, and increases in both flow and tidal elevation occur during the late fall and winter months (Jay et al. 2015). This is highly relevant to the level of inundation that could occur from the combined events. The boundary condition inputs for the hydrodynamic model were Grays River stream flow and tidal elevations at Grays Bay (Fig. 1). We obtained streamflow data from the Grays River gage station (ID 25B060) from the Washington Department of Ecology (WDOE) (H. Christensen, personal communication, April 1, 2008) for the period of record, including the H-POM analysis period from June 2006 through February 2007 (Fig. 3a). Note that flows above approximately 147 $m^3 s^{-1}$ were estimated by WDOE. The largest measured discharge was 75.9 $m^3 s^{-1}$ for developing the stage-flow rating curve (H. Christensen, personal communication, April 17, 2006). Larger discharge estimates were based on the floodplain cross section at the gage station. The flow records for Grays River show a distinct dry period during the summer and early fall of 2006 when the flows were less than 20 $m^3 s^{-1}$. This low-flow period lasted until early November 2006, at which time there was an abrupt change to a wet period during which flows

peaked at 467 $m^3 s^{-1}$ on 7 November 2006. Several smaller peak flow events occurred during the remainder of the H-POM analysis period (Fig. 3a). These episodic peaks in streamflow are the result of winter storms, which result in varying levels of floodplain inundation.

We obtained water-level data for the Columbia River and near Grays Bay, Washington, from the National Oceanic and Atmospheric Administration (NOAA) station near Astoria, Oregon, at Tongue Point (ID 9439040) located approximately 6.4 km southwest of Grays Bay. Data from this station include the effects of upstream flow from Bonneville Dam releases as well as tidal influences. We also acquired tidal predictions for Harrington Point, Washington, the station closest to Grays Bay, using the NOAA tide prediction software to provide the water-level time series for Grays Bay. The largest estimated elevations in Grays Bay were approximately 3.0 m North American Vertical Datum 1988 (NAVD88) and the minimum elevations were approximately -0.5 m NAVD88, giving a maximum tidal range of about 3.5 m. Comparison of the Grays River flows (Fig. 3a) and the tidal elevation plots (Fig. 3b) shows that the largest flows in the Grays River occurred during a period characterized by large tidal range and corresponding high tidal elevations. That is, the largest tidal elevations occur during periods of greatest flow.

The investigation of flooding in the Grays River by Breithaupt and Khangaonkar (2008) and Breithaupt and Lee (2011) included calibration of the model to WSEs measured at the KF site (locations shown in Fig. 1b). Subsequent FVCOM model predictions visibly closely matched the measured water levels at the sensor locations in and near the site (Fig. 4). While the vertical datum of the WDOE gage was arbitrary, the trend of modeled WSE matched that of the measured stage. In general, these comparisons indicated that the model represented the water-surface variations and the hydrodynamics of the Grays River over the whole model domain, thereby validating the model.

Vegetation and H-POM Flux

We used vegetation data from the KF site to calibrate the biomass transport component of the model. We collected the above-ground herbaceous biomass density from 0.1 m^2 plots located within 23 of the 127 random 1.0 m^2 vegetation cover plots in the 4,800 m^2 sampling area. This sampled area was reasonably representative of the vegetation community over the majority of the site. For each sample plot, we clipped all live and dead vegetation, rinsed the sample over a 1–2 mm mesh sieve, dried (~104°C) the sample until its weight did not change, and weighed the

sample after cooling. During the June 2006 summertime maximum, the average dry-weight biomass density was 0.78 kg m^{-2} (n = 23). During the February 2007 winter senescent period, the estimated biomass density from the same sampling area using the same methods was 0.37 kg m^{-2} (n = 22), indicating a loss of 0.41 kg m^{-2} (52%) over the 246-day interval. We assume that this loss was from export, not on site decomposition or grazing. For comparison, two other times we sampled biomass and computed flux at the KF site using the same methods used in 2006/2007. From summer 2005 to winter 2006, the flux estimate was 0.38 kg m^{-2} (64%), and during summer 2009 to winter 2010, the flux estimate was 0.66 kg m^{-2} (65%). Within year and plot, range in above-ground biomass density was high (i.e., on the order of 80% of the mean; our unpublished data). However, we felt that the mean dry-weight biomass density changes between winter and summer represented a reasonable estimate of central tendency for our overall flux estimates. The estimate of the material flux used in model calibration lie within the 95% confidence interval around the mean for the three samplings (0.44 +/- 0.24 kg m^{-2}). The field measurement of mean biomass loss was used was used to calibrate the H-POM model to produce the estimated loss of biomass due to fluid shear stress on standing biomass during inundation periods between June 2006 and February 2007 (see Appendix S1).

The vegetation biomass calibration was conducted in two steps to reduce the number of iterations of complete 246-day simulations. For both steps, the calibration was done on an area corresponding to the size and location of biomass sampling (Fig. 2c). The first step involved simulation over a 2-week period (late October 2006) during the dry period and a 4-week period (November 2006) during the wet period. We extrapolated the loss results for this short-duration simulation to the entire H-POM analysis period. We adjusted the loss rate coefficient until the extrapolated biomass loss from the model was close to the measured biomass density loss of 0.41 kg m^{-2}. After this adjustment, the second step was a simulation over the complete 246 days between June 1, 2006 and February 28, 2007. This second step confirmed that the modeled biomass loss using the extrapolated loss rate coefficient produced a result similar to the measured biomass loss.

For the H-POM flux analysis, we specified an initial biomass density of 0.78 kg m^{-2} for the entire KF site (Fig. 5a, blue background). We computed the flux from the biomass density loss, which provided the upper bound of biomass available for transport. To calculate the H-POM flux at the KF site from biomass density loss, the average biomass density over the restoration area at

hourly intervals was multiplied by the area of the KF site to compute total biomass remaining, and the difference between biomass over each interval provided the average transport (kg s^{-1}) from the whole KF site for each hourly interval. In the model, loss is a function of the constant coefficient, variable velocity, and variable depth; therefore, channels are the areas where the H-POM loss is greatest, and less is lost from the central parts of the site that are farthest from the channels. Although the biomass was set as constant across the site despite the certainty of spatial variation, these physics-based variations across the site in the model produced a large downward reduction in the estimated flux.

After mobilization of the H-POM within the KF site during inundation, the model transported H-POM through the water column into Seal Slough, the Grays River, and wetland channels. Grid cells became wet and dry as tidal elevations and river discharge changed. H-POM was stranded when a grid cell became dry. H-POM flux through the water column was computed as the mass of H-POM passing through a boundary line (i.e., transect) at hourly intervals.

To simulate H-POM flux, we used the sediment transport model in FVCOM version 2.5.3, with the following assumptions (see also Appendix S1): 1) Because no base flow enters Seal Slough from tributary streams, during dry conditions all of the flow is due to tidal exchange. 2) Settling of H-POM from the water column does not occur during transport; however, H-POM can become stranded in grid cells that have dried after floodwaters have subsided or the tide has receded. 3) Plant biomass density data from vegetation sampling plots within 100 m of the main channel at the KF site were considered representative of biomass for the site. Some of the site had been classified as wet pasture in the U.S. Fish and Wildlife Service National Wetlands Inventory prior to restoration. Only the above-ground herbaceous and leafy portion of the vegetation at the KF site was included in the analysis, not loss or transport of woody debris. 4) The H-POM mass loss from the vegetation can be approximated using a functional relation between fluid velocity, bed shear stress, and mass loss, the form of which is the same for that of sediment transport. Calibration of the model to POM loss was made using a median particle size of 0.6 mm. 5) All of the plant biomass lost between summer and late winter was mobilized as H-POM. After being stripped from the vegetation, the transport of H-POM was determined by the transport equation and there was no loss from H-POM decay.

To evaluate the potential capture of H-POM in various locations in the floodplain due to stranding, three transects across the floodplain and channels were established in the model

downstream of the KF site (Fig. 2d). We calculated H-POM flux through the system at hourly intervals at four locations: 1) at the KF site, 2) downstream of the KF site (Below KF transect), 3) downstream of the confluence of Seal Slough with the Grays River (Confluence transect), and 4) at the mouth of the Grays River (Mouth transect). Total flux across each transect was computed by summing the individual cell-face fluxes at hourly intervals. The velocity of each grid cell was multiplied by the width and average depth at each cell face to estimate flow ($m^3\ s^{-1}$) through the cell face. The average H-POM concentration ($kg\ m^{-3}$) at the grid cell face was multiplied by the flow to compute H-POM mass flux ($kg\ s^{-1}$) through each cell face. Negative values indicated that flow was outward from the system (i.e., downstream from the KF site). Values in cells along the transect were summed to compute total transport of H-POM through the system.

Assumptions

We assumed the following: (1) the OM behaves similarly to inorganic matter in that sediment transport processes are similar; (2) OM decay is not included in the model but would be expected to be most significant within the model domain in those regions where OM is stranded; while the OM transported in the pulses down the channel into the Columbia River would not be so significant because of the short, in-channel transport time during the flood pulse; (3) removal/erosion of the OM from the restoration site implicitly includes removal of OM from restoration-site vegetation throughout the water column; and, (4) the density of OM is low enough to prevent significant settling through the water column so that stranding becomes the primary loss from fluid transport. We offer that each of these assumptions should be evaluated in future research, which should include further review of available literature and potentially laboratory or field studies.

Results

Above-ground herbaceous vegetative biomass density at the KF site decreased over the simulation period between June 2006 and February 2007 (Fig. 5a-c). At three times during the simulation, the cumulative H-POM mass change was partitioned between the channels and the floodplain: 3 November 2006, 8 November 2006, and 16 February 2007 (Table 1). Prior to peak flooding, mobilization of H-POM mass at the KF site was notable (27.4×10^3 kg), but featured

very little mass transport out of the site. The largest biomass losses occurred during the wet period between early November 2006 and mid-February 2007, primarily during riverine flooding events when high flows entered the KF site at the northeast corner and exited through dike breaches and the west-side culverts. After the peak flooding period, cumulative H-POM mobilization had increased to 76.2×10^3 kg, and a total of 22.0×10^3 kg of H-POM was transported through the Below KF transect. Of the transport through this transect, about 21% (4.54×10^3 kg) of the H-POM flux was through Seal Slough, and the bulk of H-POM transport was down the Grays River or over the floodplain. At the Confluence transect, the bulk of H-POM transport was down the Grays River (96%), and a little H-POM flux occurred over the floodplain. During the peak flood there was only a short period during which the dike along the south bank of Seal Slough was overtopped, and only 4% of the H-POM mass transport washed through the floodplain portion of the transect.

The spatial distribution of H-POM concentration also changed over the simulation period due to loss of biomass from the KF site and its transport downstream (Fig. 5d-f; Video S1). At the onset of the simulation (hour 1, Fig, 5b), H-POM concentrations were negligible due to the initial concentration being set to zero and the short duration of simulation up to this time. By the end of the dry period and before the onset of the wet period in November 2006, H-POM concentration had increased within the KF site, increases in H-POM concentration in Seal Slough and the Grays River were negligible (Fig. 5e). During the dry period, tidal exchange was the dominant driver of the mobilization and redistribution of H-POM within the KF site, and little H-POM was exported from the site. Export occurred only after the onset of the wet period in November 2006.

The peak flood in the Grays River during November 2006 was followed by episodes of high flow in the Grays River through February 2007 (Fig. 3a), and both produced a greater range of inundation within the site. The periods of high flows through the KF site have larger bed shear stress, which mobilizes more H-POM, transports it from the KF site into Seal Slough and the Grays River, and carries it downstream (Fig. 5f). Because floodwaters inundate the floodplain, as well as the KF site, H-POM became distributed across most of the floodplain downstream (Fig. 5f). Exceptions were areas behind dikes. As floodwaters receded, H-POM was stranded at locales that became dry. Tidal exchange or later floodwater was able to transport stranded H-POM farther through the system. Some H-POM was transported upstream (northeast) from the KF site (Fig. 5f) by flood tides, which caused flow reversals in Grays River.

Instantaneous flow across the three H-POM flux transects (Fig. 2d) varied according to tidal forcing and pulsed periods of flow driven by strong flood events (Fig. 6a, b). Prior to November 2006, the flow across transects was essentially in balance and tidal exchange dominated the system's hydrodynamics. The peak flood event of the simulation period was composed of two events separated by about 12 hours in early November 2006, and other smaller floods occurred later during the late fall and winter. The peak flood overtopped the dike upstream (northeast) of the KF site, which resulted in a flush of floodwater through the site. During this event and the remainder of November 2006, net flows at all transects were directed downstream (negative flows). After mid-January 2007 the flow returned to conditions similar to the period prior to the peak flood (largely tidally dominated). Note the increase in tidal exchange from upstream (Below KF transect) to downstream (Mouth transect) as indicated by the larger range of flows (Fig. 6a, b).

The largest instantaneous H-POM flux was at the KF site and the smallest was at the Mouth transect (Fig. 6c). At the KF site, the pulses of increased flux prior to the peak flood did not result in transport downstream, but instead any H-POM entrained in the water column was redistributed around the KF site (Fig. 5e). It was not until the peak flood event that transport occurred through the downstream transects. After the pulse of efflux during the peak flood event, the Confluence transect (Fig. 2d) exhibited oscillating transport (Fig. 6c), with positive (inflow) and negative (outflow) exchange, indicating net H-POM flux from the system was reduced. We attribute this to the reduction in outflow after mid-January 2007 (Fig. 6a, b).

Closer examination of the H-POM flux with the onset of the wet period and around the period of the peak flood revealed changes in the magnitude of flux and changes in the relative spatial distribution of fluxes at transects downstream (Fig. 6b). During this period, river flows increased, resulting in larger inundations of the KF site at flood tides that produced large spikes in H-POM mobilization. As the peak floodwaters overtopped dikes downstream and began flowing through the KF site on 6 November 2006, H-POM flux at the KF site continued to respond to tidal exchange, but the additional influence of the floodwaters produced longer periods of mobilization. The increased H-POM flux from the KF site produced increased flux through the Below KF transect, which was followed by smaller increases in fluxes at transects downstream of the Confluence transect during tidal ebb, although H-POM flux at the Mouth transect increased only slightly. A larger pulse of H-POM flux occurred on 7 November 2006

with the passage of the flood peak at the KF site, and sequentially decreasing magnitudes occurred through each downstream transect. This decrease is attributed to storage due to stranding in the Grays River system, i.e., the floodplain and channels.

The peak flood produced H-POM mass change at the four locations and a sharp increase in cumulative H-POM loss from the system (i.e., negative mass change), and by the end of the simulation approximately 94.2×10^3 kg of H-POM had been mobilized at the KF site (Fig. 6c). At the Below KF transect, the estimated cumulative H-POM mass change was approximately 96.2×10^3 kg. At the Mouth transect, 49.6×10^3 kg (52%) of H-POM had been transported from one wetland in the Grays River into Grays Bay by the end of the simulation. The remaining 46.6×10^3 kg (48%) of H-POM was deposited in the Grays River and floodplain.

We attribute the slightly larger value of mass mobilized at the Below KF transect relative to the KF site to the difference in methods (mass loss rates at the KF site and mass transfer rates across each transect) used to calculate flux at the KF site and the other three locations. The difference in error between the methods is approximately 2% and often negligible. The internal computations of the models were made at 5-second time steps while the results are given at hourly intervals. Variations in velocity and H-POM concentrations at intervals smaller than 1 hour are likely, which could produce cumulative errors in flux estimates. However, the overall trend shows the mass change was smaller at the Below KF, Confluence, and Mouth transects than the mass mobilized at the KF site. There was a decrease between each successive transect downstream (Fig. 6c), which is attributed to storage in the Grays River system floodplain and channels. The Confluence transect exhibited no further increase after mid-January 2007, which is attributed to the change in flow regime (Fig. 6a) and the oscillatory H-POM flux (Fig. 6b).

In summary, according to the model, the fate of biomass produced per unit area at the site breaks down as follows (Fig. 7): 1) Peak summer biomass density at the KF site averaged 0.78 kg m^{-2}, which equals a total of 506.4×10^3 kg for the entire 65 ha site. 2) Biomass reduction due to H-POM mobilization equaled 0.301 kg m^{-2} or 38.7% of the peak summer biomass density (i.e., this value represents the portion of the lost biomass that was mobilized). 3) Biomass not mobilized equaled 0.478 kg m^{-2} or 61.3% of the peak summer biomass density. 4) Mobilized H-POM retained on the site equaled 0.153 kg m^{-2} or 19.6% of the peak summer biomass density, and 50.8% of all mobilized H-POM. 5) Mobilized H-POM exported equaled 0.148 kg m^{-2} or 19.0% of the peak summer biomass density, and 49.2% of all mobilized H-POM. 6) Mobilized

H-POM retained in the Grays River and floodplain equaled 0.071 kg m^{-2} or 9.1% of the peak summer biomass density, and 48.0% of all exported H-POM. 7) Mobilized H-POM distributed to the main stem Columbia River estuary equaled 0.077 kg m^{-2} or 9.9% of the peak summer biomass density, and 52.0% of all exported H-POM. This demonstrates that enhanced hydrological connection to a formerly diked wetland resulted in transport of H-POM from the KF site to the floodplain, main stem river, and estuary.

Discussion

Restoring an ecosystem function such as H-POM export is among a set of paradigms commonly put forward as drivers of ecosystem recovery (Duarte et al. 2013a). The mass-transport modeling in this study demonstrated that POM produced in a tributary floodplain wetland cumulatively affects the main stem estuary 7 km downstream, nearby restoration sites, and even areas upstream of the wetland through tidal reversals. These indirect and cross-boundary effects (CEQ 1997; Diefenderfer et al. 2016) occurred throughout the floodplain riverscape. The modeling showed that the new culverts, as well as a flood event that overtopped the levee, were important conduits for the exchange of a large mass of organic material. This supports the hypothesis that restoring hydrological connections is a viable strategy for enhancing marsh macrodetritus contributions to the food web in the Columbia River estuary (Maier and Simenstad 2009).

Limitations of Results

Although we did not conduct a similar simulation for the conditions with the tide gate in place, we assume that exchange was far less than with the new culverts based on the relative dimensions of the openings, the elevation of the tide gate, and the dampening effect of its lid. According to our post-construction modeling, between summer and mid-winter, approximately 96.2×10^3 kg of H-POM was exported downstream of the KF site. Of this mobilized H-POM, 100% passed the Below KF transect, 65% passed through the Confluence of Seal Slough and the Grays River, and about 52% passed through the mouth to Grays Bay (Figure 2d), which is located on the main stem of the Columbia River in the estuary system zone (Jay et al. 2016). H-POM was redistributed to the floodplain during the peak flood events, and was then available for transport during moderate flow conditions. The mobilized H-POM that was not transported

463 through a sampling transect was apparently stored in the Grays River system floodplain and
464 channels, and was presumably susceptible to transport downstream in future events until further
465 breakdown or uptake of materials occurred.
466
467 *Marsh Plant Community*
468 Mobilization of vegetation depends on a variety of factors (i.e., death, fragmentation, and
469 decay) some of which are not taken into account in our model. For example, the breakdown of
470 reed canarygrass is complex in that stems may or may not die over the winter and that the stems
471 can re-sprout in the spring even after appearing to be dead in the winter (leaves generally die
472 every year). Ultimately the whole 1–2 m tall plant dies and falls over, and may or may not form a
473 dense mat. In any case, the stems begin to break down and, over the course of a year, break into
474 increasingly smaller pieces. The stem fragments initially float because they are hollow.
475 Eventually the stems become waterlogged and sink, but we are not sure how long that takes. We
476 used biomass loss data from the site during the period for which the model was run, thereby
477 capturing the bulk of the vegetation being mobilized and transported. That said, further study is
478 warranted to partition the contribution of floating and waterlogged fragments to H-POM fluxes
479 and fate.
480 Variability in biomass production and loss is significant in the Columbia River estuary. Our
481 estimate of the summer vascular plants standing crop (0.78 kg m^{-2}) from data collected at the KF
482 site is within the range reported by Small et al. (1990) of 0.27 to 1.65 kg m^{-2}. Like Small et al.
483 (1990), who sampled several sites in the lower estuary, our data on H-POM production on
484 similar high marshes on the Columbia floodplain indicate a very high range and variability of
485 macrodetritus production: minimum = 0.03, maximum = 1.59, median = 0.72 kg dry weight m^{-2}
486 yr^{-1} for 32 sampling areas across 7 sites over 5 years (A. Borde, unpublished data, PNNL,
487 Sequim, WA). Data for the KF and two other restoration sites and their paired reference sites are
488 also highly variable between sites, within sites, and among years (Diefenderfer et al. 2016).
489 Based on observations of the entire KF site over many years, we believe that the variability in
490 production across the site, which we simplified to a single estimate based on subsampling of one
491 part of the site, is also dwarfed by the variability throughout the ecosystem such that the
492 simplification for modeling purposes is irrelevant. Our long-term sampling of sites has shown
493 that high variability in annual production in these marshes is driven by seasonal and interannual

494 variability in hydrologic conditions (Borde et al. 2013). In addition, the range of plant biomass
495 density during summer and in winter in reference marshes indicates that much higher or lower
496 quantities may be produced and lost in some sites, parts of sites, or years. Based on these
497 additional data from across the floodplain and our modeling, we conclude that, in general,
498 detritus is exported from restoration sites on tributaries to nearby wetlands and perhaps over
499 longer distances to the main stem over a larger inference space, i.e., restoration and reference
500 marshes on the tidally influenced Columbia River floodplain.
501 Simenstad et al. (1990) estimated for the Columbia estuary that herbivores remove 15% of
502 annual emergent plant carbon production, and that translocation to the roots removes 38%,
503 leaving approximately 47% to enter the H-POM pool. For the Fraser River tidal delta in southern
504 British Columbia, Kistritz et al. (1983) showed that approximately 37% of the sedge marsh
505 biomass was exported off the marsh plain annually, and that virtually all of that took place
506 during winter. Our measurements and model only treated the potential H-POM pool and we did
507 not measure loss via herbivory, translocation, or burial. Our estimate that 19% of the annual
508 emergent plant carbon produced is exported is somewhat low compared to these other regional
509 estimates. We wonder if this may be due to differences in wetland species. After hydrological
510 connection, the KF site became dominated by reed canarygrass, a species that develops thick,
511 tough mats that may be more recalcitrant to mobilization (e.g., Griffiths et al. 2012) than those
512 dominating sites studied by Simenstad et al. (1990) and Kistritz et al. (1983), e.g., *Carex*
513 *lyngbyei*. Reed canarygrass has a faster decomposition rate than *Typha latifolia* (common
514 cattail), *Juncus effusus* (soft rush), and *Alnus rubra* (red alder) leaves (Gingerich and Anderson
515 2011), which are common elsewhere including in other parts of the Columbia River estuary.
516 Additionally, the model only removes POM via physical means (erosion and transport), which
517 are governed by fluid motion, and produces the greatest velocity and potential for erosion in the
518 channels. The model does not include biological processes that would lead to losses observed in
519 the field in areas distant from channels, which do not show losses in this modeling (Fig. 5f). In-
520 channel transport would have limited time for decay before H-POM is flushed into the Columbia
521 River. The stranded OM would be subject to decay within the modeling analysis domain. The
522 stranded H-POM could be flushed and transported further depending on the recurrence rate and
523 size of flood pulses. This is consistent with efforts by others who have shown that biogenic
524 influences on physical processes increase farther from marsh channels (Collins et al. 1987).

525

526 *Ecosystem Connectivity and Spatial Subsidies of Restoration*

527 While delivery of H-POM to estuaries and near-coastal systems is generally viewed as a key
528 aspect of global biogeochemical cycles, the role of storm-driven pulsed delivery is less well
529 appreciated (Hope et al. 1997; Mooney and McClelland 2012). We believe that the pulsed
530 redistribution of H-POM in the Grays River floodplain and channels and then to the main stem
531 Columbia River in the estuary zone is an important nuance associated with defragmentation of
532 estuarine ecosystems through restoration of hydrological interconnections. Climatic fluctuation
533 resulting in variation in winter flood magnitude and frequency, or changes to the level of ocean
534 water relative to land elevation, thus may regulate detrital pathways throughout the ecosystem.
535 Notably, the transport of material to adjacent elements of the riverscape, including other
536 restoration sites in the model domain, suggests that the effect of multiple hydrologic
537 reconnections in a riverscape could be synergistic, as previously demonstrated (Diefenderfer et
538 al. 2012). This "lateral" connectivity (Amoros and Bornette 2002) demonstrates the spatial
539 subsidy of organic matter (Summerhayes and Elton 1923; Polis et al. 1997), an important process
540 contributing to a wide array of ecosystem functions (Naiman and Décamps 1997; Nakano and
541 Murakami 2001). Alone, however, lateral connectivity stops short of describing changes in the
542 receiving system, i.e., "functional" connectivity (Talley et al. 2006). Further research remains to
543 be done in the Columbia River estuary and other systems to elucidate the fate of material relative
544 to environmental conditions such as seasonal temperature and flow and the temporal aspects of
545 specific mechanisms by which material is taken up in the food web.
546
547 It is clear from studies in other systems that detritus from vascular plants and associated
548 algae contributes to production of prey for estuarine-dependent fish species (e.g., Odum and
549 Heald 1975; Nixon 1980; Boesch and Turner 1989). With recent information showing that the
550 prey consumed by estuarine-dependent juvenile salmon in the Columbia use marsh detritus as a
551 major source of energy (Maier and Simenstad 2009), our rough estimate of H-POM export to the
552 estuary, not including aged detrital material export, provides guidance on the magnitude and type
553 of restoration actions that could begin to have a significant effect on restoring the broader
554 estuarine food web that is important to young salmon in the ecosystem. The mass-transport
555 modeling also reinforces other evidence that the detrital-based part of the salmonid food web of

the Columbia River estuary is shaped by multiple sources and pathways from outside the main stem estuary (Maier and Simenstad 2009; Naiman et al. 2012). Moreover, Kukulka and Jay (2003) showed that diking and flow regulation have reduced the opportunity for shallow-water habitat access by young salmon by 62% during the critical freshet period. Simenstad et al. (2000) concluded that landscape structure and scale are important when designing restoration projects to benefit coastal and estuarine fishes that use shallow-water habitats. In the case of the Columbia River estuary, access to preferred prey resources depends on both direct access to shallow-water habitats and, under altered conditions, access to prey in main stem estuary portions of the system (Diefenderfer et al. 2016). Under these altered conditions, salmon access to prey feeding on marsh macrodetritus may depend more on H-POM exported to deeper areas than previously thought. Larger fish that may infrequently enter shallow tidal channels can still benefit from H-POM produced and exported from wetlands, especially if that flux includes insect prey.

Our estimate of total production by marsh macrophytes in the KF site was 5.32×10^5 kg, which equals 2.13×10^5 kg C (i.e., using the conversion factor 1 g biomass = 0.4 g C employed by Small et al. 1990). Thus, the KF site production represented about 2% of the total marsh macrophyte production estimate (1.13×10^7 kg C) made by Small et al. (1990) for the entire estuary. The 65 ha KF site represents 0.67% of the 9,747 ha of tidal herbaceous wetland lost from the system since the late 1800s (Marcoe and Pilson 2017). Scaling up to the broader estuary, we multiplied this yield estimate by the 9,747 ha of herbaceous wetlands lost and by the estimate that 23% of the macrophyte production that is exported. Our calculation resulted in an estimated annual loss of 7.35×10^6 kg C (= 3.28×10^3 kg C × 9,747 ha × 0.23) to the ecosystem compared with roughly 24×10^6 kg C lost annually in the late 1800s.

Diefenderfer et al. (2016) found that sediment accretion occurred after the levee breach, and contributed to restoring the elevation and vegetation structure of the subsided marsh plain at the KF site. At the same site, we found that pulsed flood events drove export of substantial amounts of POM and probably some sediment, marsh-associated invertebrates, and dissolved organic matter. Considering these results, hydrologically reconnecting a wetland to its main stem river not only results in wetland recovery it also results in re-establishing support to the system downstream, including, in this case, the main stem of the Columbia River estuary.

Conclusion

The processes of primary production and exchange of organic matter are of fundamental importance to maintaining the flow of energy among elements of the ecosystem, and material flux is essential for supporting the food web, biodiversity, and production of prey. Management plans that result in modification of the supply of organic matter to riverine, estuarine, and coastal food webs need to consider the effects of changes in the system on the amount and mix of the organic matter supply (e.g., Jassby et al. 1993; Sobczak et al. 2002; Hunsinger et al. 2010). Changes in the hydrodynamics of river systems are also relevant because, as we have shown, H-POM flux can be driven by river discharges that inundate the floodplain, while tidal exchange at low flows contribute less to flux. We believe that further studies aimed at quantifying this organic matter flow as a functional response to habitat restoration projects and pulsed events in the physical environment would prove a clear link between restoration actions and ecosystem services. Developing estimators of the effects of multiple actions on the restoration of organic matter flow will assist in quantification of the cumulative effects of multiple restoration projects on an ecosystem, perhaps one of the most daunting and relevant problems in restoration ecology. Modeling methods such as those demonstrated herein have the potential to help assess and predict material fluxes in hydrologically dynamic zones and evaluate landscape-scale effects attributable to the fragmentation or reconnection of terrestrial-aquatic ecosystems.

Acknowledgements

The research reported here was funded by the Portland District of the U.S. Army Corps of Engineers under the Columbia River Fish Project. We sincerely thank the late Blaine Ebberts, and Cindy Studebaker, of the Portland District for their support, encouragement, and direction of the research. We are grateful to the Columbia Land Trust, Vancouver, Washington, for permitting us to conduct research on wetlands that it conserved and restored on the Grays River. Taeyun Kim assisted with the model application and Luca Castrucci assisted with model extractions and aerial imagery overlays. Nathan Johnson provided overall graphics support. Field and logistical support were provided by Earl Dawley and Alan Whiting. Shannon Bates and Susan Ennor edited the final draft. Finally, we thank John Vavrinec, Bob Christian, Clayton Williams, Christer Nilsson and two anonymous reviewers for providing very helpful comments on various versions of the manuscript.

617 **Literature Cited**

618 Amoros, C., and G. Bornette. 2002. Connectivity and biocomplexity in waterbodies of riverine
619 floodplains. Freshwater Biology 47:761-776.
620 Boesch, D. F., and R. E. Turner. 1984. Dependence of fisheries species on salt marshes: The role
621 of food and refuge. Estuaries 7:460-468.
622 Borde, A. B., S. A. Zimmerman, R. M. Kaufmann, R. M. Thom, and C. L. Wright. 2013. Lower
623 Columbia River and Estuary Habitat Monitoring Study: 2012 Annual Report. PNNL-22410.
624 Prepared for the Lower Columbia River Estuary Partnership by Pacific Northwest National
625 Laboratory, Richland, Washington.
626 Breithaupt, S., and T. Khangaonkar. 2008. Forensic Hydrodynamic Evaluation Following the
627 Restoration of a Tidal Freshwater Wetlands. Estuarine and Coastal Modeling. doi:
628 10.1061/40990(324)34.
629 Breithaupt, S. A., and C. Lee. 2011. Hydrodynamic Modeling Analyses for the Mill Road
630 Restoration Project, Grays River, Washington. PNWD-4245. Prepared for Columbia Land
631 Trust, Vancouver, WA.
632 Chen C., R. C. Beardsley, and G. Cowles. 2006. An Unstructured Grid, Finite-Volume Coastal
633 Ocean Model, FVCOM User Manual. SMAST/UMASSD-06-060, University of
634 Massachusetts-Dartmouth, Dartmouth, Massachusetts.
635 Childers, D. L., J. W. Day Jr., and H. N. McKellar Jr. 2000. Twenty more years of marsh and
636 estuarine flux studies: revisiting Nixon (1980). In Concepts and controversies in tidal marsh
637 ecology, eds. Michael P. Weinstein and Daniel A. Kreeger, 391-423. Dordrecht, Netherlands:
638 Kluwer Academic Publishers.
639 Collins, L. M., J. N. Collins, and L. B. Leopold. 1987. Geomorphic processes of an estuarine
640 marsh. Pages 1049–1072 in V. Gardiner (ed.), International Geomorphology 1986: Part I.
641 Proceedings of the First International Conference on Geomorphology. John Wiley & Sons
642 Ltd., Hoboken, New Jersey.
643 Council on Environmental Quality (CEQ). 1997. Considering cumulative effects under the
644 National Environmental Policy Act. Executive Office of the President, Washington, D.C.
645 Correll, D.L. 1978. Estuarine productivity. BioScience 28:646-650.
646 Dahm, C. N., S. V. Gregory, and P. K. Park. 1981. Organic carbon transport in the Columbia
647 river. Estuarine, Coastal Shelf Science 13:645-658.

Dame, R., T. Chrzanowski, K. Bildstein, B. Kjerfve, H. McKellar, D. Nelson, J. Spurrier, S. Stancyk, H. Stevenson, J. Vernberg, and R. Zingmark. 1986. The outwelling hypothesis and North Inlet, South Carolina. Marine Ecology Progress Series 33:217-229.

Diefenderfer, H. L., A. M. Coleman, A. B. Borde, and I. A. Sinks. 2008. Hydraulic geometry and microtopography of tidal freshwater forested wetlands and implications for restoration, Columbia River, U.S.A. Ecohydrology & Hydrobiology 8:339-361.

Diefenderfer, H. L., G. E. Johnson, J. R. Skalski, S. A. Breithaupt, and A. M. Coleman. 2012. Application of the diminishing returns concept in the hydroecologic restoration of riverscapes. Landscape Ecology 27:671-682.

Diefenderfer, H. L., G. E. Johnson, R. M. Thom, K. E. Buenau, L. A. Weitkamp, C. M. Woodley, A. B. Borde, and R. K. Kropp. 2016. Evidence-Based Evaluation of the Cumulative Effects of Ecosystem Restoration. Ecosphere 7(3): Article e012421.

Diefenderfer H. L., R. M. Thom, G. E. Johnson, J. R. Skalski, K. A. Vogt, B. D. Ebberts, G. C. Roegner, and E. M. Dawley. 2011. A levels-of-evidence approach for assessing cumulative ecosystem response to estuary and river restoration programs. Ecological Restoration 29:111–132.

Duarte, C. M., A. Borja, J. Carstensen, M. Elliott, D. Krause-Jensen, and N. Marbá. 2013a. Paradigms in the recovery of estuarine and coastal ecosystems. Estuaries and Coasts DOI 10.1007/s12237-013-9750-9.

Duarte, C. M., I. J. Losada, I. E. Hendriks, I. Mazarrasa, and N. Marbá. 2013b. The role of coastal plant communities for climate change mitigation and adaptation. Nature Climate Change 3:961-968.

Ebberts B. D., B. D. Zelinsky, J. P. Karnezis, C. A. Studebaker, S. Lopez-Johnston, A. M. Creason, L. Krasnow, G. E. Johnson, and R. M. Thom. 2017. Estuary ecosystem restoration: Implementing and institutionalizing adaptive management. Restoration Ecology. doi: 10.1111/rec.12562

Emmett, R., R. Llanso, J. Newton, R. Thom, M. Hornberger, C. Morgan, C. Levings, A. Copping, and P. Fishman. 2000. Geographic signatures of North American west coast estuaries. Estuaries 23:765-792.

Gingerich, R. T., and J. T. Anderson. 2011. Decomposition trends of five plant litter types in mitigated and reference wetlands in West Virginia, USA. Wetlands, 31:653-662.

679 Griffiths, N.A., J.L. Tank, S.S. Roley, and M.L. Stephen. 2012. Decomposition of maize leaves
680 and grasses in restored agricultural streams. Freshwater Science 31:848-864.
681 Haines, E.B. 1977. The origins of detritus in Georgia salt marsh estuaries. Oikos 29: 254-260.
682 Healy, M.C. 1979. Detritus and juvenile salmon production in the Nanaimo estuary: I.
683 Production and feeding rates of juvenile chum salmon. J. Fish. Res. Board Can. 36:488-496.
684 Hope, D., M. F. Billett, R. Milne, and T. A. W. Brown. 1997. Exports of organic carbon in
685 British rivers. Hydrological Processes 11:325-344.
686 Hunsinger, G. B., S. Mitra, S. E. G. Findlay, and D. T. Fischer. 2010. Wetland-driven shifts in
687 suspended particulate organic matter composition of the Hudson River estuary, New York.
688 Limnology and Oceanography 55:1653-1667.
689 Irving, A. D., S. D. Connell, and B. D. Russell. 2011. Restoring coastal plants to improve global
690 carbon storage: reaping what we sow. Plos One 6:1-3.
691 Jassby, A. D., J. E. Cloern, and T. M. Powell. 1993. Organic carbon sources and sinks in San
692 Francisco Bay: Variability induced by river flow. Marine Ecology Progress Series 95:39-54.
693 Jay, D. A., A. B. Borde, and H. L. Diefenderfer. 2016. Tidal-fluvial and estuarine processes in
694 the lower Columbia River: II. Water level models, floodplain wetland inundation, and reach
695 classification. Estuaries and Coasts 39:1299-1324.
696 Jay, D. A., K. Leffler, H. L. Diefenderfer, and A. B. Borde. 2015. Tidal-fluvial and estuarine
697 processes in the lower Columbia River: I. Along-channel water level variations, Pacific
698 Ocean to Bonneville Dam. Estuaries and Coasts. 38:415-433. doi 10.1007/s12237-014-9819-
699 0 published online 2014.
700 Johnson, G. E., and J. J. Gonor. 1982. The tidal exchange of *Callianassa californiensis*
701 (*Crustacea, Decapoda*) larvae between the ocean and the Salmon River estuary, Oregon.
702 Estuarine Coastal and Shelf Science 14:501-516.
703 Junk, W. J., P. B. Bailey, and R. E. Sparks. 1989. The flood pulse concept in river-floodplain
704 systems. Canadian Special Publication of Fisheries and Aquatic Sciences 106:110-127.
705 Ke, Y., A. M. Coleman, and H. L. Diefenderfer. 2013. Temporal land cover analysis for net
706 ecosystem improvement. Ecohydrology and Hydrobiology 13:84-96.
707 Kistritz, R. U., K. J. Hall, and I. Yesaki. 1983. Productivity, detritus flux, and nutrient cycling in
708 a *Carex lyngbyei* tidal marsh. Estuaries 6:227–236.

709 Kukulka, T. and D. A. Jay. 2003. Impacts of Columbia River discharge on salmonid habitat 2:
710 Changes in shallow-water habitat. Journal of Geophysical Research 108(C9):3294.
711 Maier, G. O. and C. A. Simenstad. 2009. The role of marsh-derived macrodetritus to the food
712 webs of juvenile Chinook salmon in a large altered estuary. Estuaries and Coasts 32:984–
713 998.
714 Maier, G. O., J. D. Toft, and C. A. Simenstad. 2011. Variability in isotopic (□13C, □15N,
715 □34S) composition of organic matter contributing to detritus-based food webs of the
716 Columbia River estuary. Northwest Science 85:41–54.
717 Mannino, A., and H. R. Harvey. 2000. Terrigenous dissolved organic matter along an estuarine
718 gradient and its flux to the coastal ocean. Organic Geochemistry 31:1611-1625.
719 Marcoe, K. and S. Pilson. 2017. Habitat change in the lower Columbia River estuary, 1870-2009.
720 Journal Coastal Conservation. Published online June 16, 2017. DOI 10.1007/s11852-017-
721 0523-7.
722 Mitsch W. J. and J. G. Gosselink. 2007. Wetlands, 4th ed. Hoboken, NJ: Wiley.
723 Mooney, R.F. and J.W. McClelland. 2012. Watershed export events and ecosystem responses in
724 the Mission-Aransas National Estuarine Research Reserve. Estuaries and Coasts. 35:1468-
725 1485.
726 Nakano, S., and M. Murakami. 2001. Reciprocal subsidies: Dynamic interdependence between
727 terrestrial and aquatic food webs. Proceedings of the National Academy of Sciences
728 98:166−170.
729 Naiman, R. J., J. R. Alldredge, D. A. Beauchamp, P. A. Bisson, J. Congleton, C. J. Henny, N.
730 Huntly, R. Lamberson, C. Levings, E. N. Merrill, W. G. Pearcy, B. E. Rieman, G. T.
731 Ruggerone, D. Scarnecchia, P. E. Smouse, and C. C. Wood. 2012. Developing a broader
732 scientific foundation for river restoration: Columbia River food webs. Proceedings of the
733 National Academy of Sciences 109:21201–21207.
734 Naiman R. J., and H. Décamps. 1997. The ecology of interfaces: riparian zones. Annual Review
735 of Ecology and Systematics 28:621−58.
736 Nixon, S. W. 1980. Between coastal marshes and coastal waters–a review of twenty years of
737 speculation and research on the role of salt marshes in estuarine productivity and water
738 chemistry. In Estuarine and Wetland Processes, P. Hamilton and K.B. MacDonald (eds.),
739 437–525. New York: Plenum Press.

Odum, H. T. 1956. Primary production in flowing waters. Limnology & Oceanography 1:102–117.

Odum, W. E. 1984. Dual-gradient concept of detritus transport and processing in estuaries. Bulletin of Marine Science 35:510–521.

Odum, W. E. and E. J. Heald. 1975. The detritus-based food web of an estuarine mangrove community. In Estuarine Research, Vol. 1, ed. L.E. Cronin, 265–286. New York: Academic Press.

Odum, W. E., E. P. Odum, and H. T. Odum. 1995. Nature's pulsing paradigm. Estuaries 18: 47-555.

Polis, G. A., W. B. Anderson, and R. D. Hold. 1997. Toward an integration of landscape and food web ecology: The dynamics of spatially subsidized food webs. Annual Review of Ecology and Systematics 28:289-316.

Roegner, G. C. 2000. Transport of molluscan larvae through a shallow estuary. Journal of Plankton Research 22:1779-1800.

Roegner G. C., H. L. Diefenderfer, A. B. Borde, R. M. Thom, E. M. Dawley, A. H. Whiting, S. A. Zimmerman, and G. E. Johnson. 2009. Protocols for Monitoring Habitat Restoration Projects in the Lower Columbia River and Estuary. U.S. Department of Commerce, National Oceanic and Atmospheric Administration Technical Memorandum NMFS-NWFSC-97, Northwest Fisheries Science Center, Seattle, Washington.

Roegner, G. C., C. Seaton, and A. M. Baptista. 2011. Climatic and tidal forcing if hydrography and chlorophyll concentrations in the Columbia River estuary. Estuaries and Coasts 34:281-296.

Sherwood, C. R., D. A. Jay, R. B. Harvey, P. Hamilton, and C. A. Simenstad. 1990. Historical changes in the Columbia River estuary. Progress in Oceanography 25:299-352.

Sibert, J. R. 1979. Detritus and juvenile salmon production in the Nanaimo estuary: II. Meiofauna available as food to juvenile chum salmon (*Oncorhynchus keta*). Journal of the Fisheries Research Board of Canada 36:497-503.

Simenstad, C. A., W. G. Hood, R. M. Thom, D. A. Levy, and D. Bottom. 2000. Landscape structure and scale constraints on restoring estuarine wetlands for Pacific coast juvenile fishes. In Concepts and Controversies in Tidal Marsh Ecology, eds. M. P. Weinstein and D. A. Kreeger, 597-630. Dordrecht: Kluwer Academic Publishers.

771 Simenstad, C. A., L. F. Small, and C. D. McIntire. 1990. Consumption processes and food web
772 structure in the Columbia River estuary. Progress in Oceanography 25:271-297.
773 Simenstad, C. A., and R. M. Thom. 1996. Functional equivalency trajectories of the restored
774 Gog-Le-Hi-Te estuarine wetland. Ecological Applications 6:38-56.
775 Simenstad, C. A., and R. C. Wissmar. 1985. $\delta^{13}C$ evidence of origins and fates of organic carbon
776 in estuarine and nearshore food webs. Marine Ecology Progress Series 22:141-152.
777 Small, L. F., C. D. McIntire, K. B. Macdonald, J. R. Lara-Lara, B. E. Frey, M. C. Amspoker, and
778 T. Winfield. 1990. Primary production, plant and detrital biomass, and particle transport in
779 the Columbia River estuary. Progress in Oceanography 25:175-210.
780 Small, L. F., and F. G. Prahl. 2004. A particle conveyor belt process in the Columbia River
781 estuary: Evidence from chlorophyll a and particulate organic carbon. Estuaries 27:999-1013.
782 Sobczak, W. V., J. C. Cloern, A. D. Jassby, and A. B. Muller-Solger. 2002. Bioavailability of
783 organic matter in a highly disturbed estuary: The role of detrital and algal resources.
784 Proceeding of the National Academy of Sciences 99:8101-8105.
785 Summerhayes, V. S., and C. S. Elton. 1923. Contributions to the ecology of Spitsbergen and
786 Bear Island. Journal of Ecology 11:214-286.
787 Talley, D. M., G. R. Huxel, and M. Holyoak. 2006. Connectivity at the land-water interface. In
788 Connectivity Conservation, eds. K.R. Crooks and M. Sanjayan, 97-129. Cambridge:
789 Cambridge University Press.
790 Teal, J. M. 1962. Energy flow in the salt marsh ecosystem of Georgia. Ecology 43:614-624.
791 Thom, R. 1984. Primary production in Grays Harbor estuary, Washington. Bulletin of the
792 Southern California Academy of Sciences 83:99-105.
793 Walsh, E. M., A. E. Ingalls, and R. G. Keil. 2008. Sources and transport of terrestrial organic
794 matter in Vancouver Island fjord and the Vancouver-Washington margin: A multiproxy
795 approach use $\delta^{13}C_{org}$ lignin phenols, and ether lipid BIT index. Limnology and Oceanography
796 53:1054-1063.
797 Wheatcroft, R. A., M. A. Goni, J. A. Hatten, G. B. Pasternack, and J. A. Warrick. 2010. The role
798 of effective discharge in the ocean delivery of particulate organic carbon by small,
799 mountainous river streams. Limnology and Oceanography 55:161-171.
800 Zedler, J. B., ed. 2001. Handbook for Restoring Tidal Wetlands. CRC Press, Boca Raton,
801 Florida.

802
803
804

805 Supporting Information

806 Additional supporting information may be found in the online version of this article at

807 http://onlinelibrary.wiley.com/doi/10.1002/eap.xxxx/suppinfo

Tables

Table 1. Cumulative H-POM mass (× 10^3 kg) change during the simulation (June 2006 – February 2007).

Negative values indicate H-POM mass exiting through the transect. The H-POM mass exiting the Mouth transect enters the main stem estuary. KF = Kandoll Farm site. See also Fig. 2d.

Time[a]	KF Site[b]	Transect: Downstream of KF Site (Below KF)				Transect: Downstream of Confluence (Confluence)			Transect: (Mouth)
		Seal Slough	Grays River	Flood-plain	Total	Grays River	Flood-plain	Total	
Prior to Peak Flood	-27.4	-0.111	-0.020	0.0	-0.131	-0.003	0.0	-0.003	0.0
After Peak Flood	-76.2	-4.54	-9.21	-8.26	-22.0	-11.9	-0.485	-12.4	-5.16
End	-94.2[c]	-1.50	-86.4	-8.29	-96.2[c]	-61.7	-0.476	-62.2	-49.6

[a] Start of simulation = 15 June 2006, 00:00; prior to peak flood = hr 3394, 3 November 2006, 10:00; following peak flood = hr 3504, 8 November 2006, 00:00; end of simulation = hr 5904, 16 February 2007, 00:00.

[b] The H-POM mass change at the KF site is the mobilization from the H-POM source.

[c] End of simulation. The difference between these two values is attributed to differences in computational methods. See text for explanation.

Figure Legends

Fig. 1 A) Location of the study area in the Columbia River estuary. The H-POM flux study was conducted at the Kandoll Farm site in the Grays River, which empties into Grays Bay. Tidal influence extends to Bonneville Dam, located at the extreme bottom right corner of the figure (not shown). B) Locations of water-level stations, the Kandoll Farm site within the Grays River watershed, and waterbody features used in the H-POM modeling analysis. KF = Kandoll Farm site, which is also the location of the culverts installed in 2005; RC = reference

channel; CH1 = channel 1, a tidal channel; WDOE = Washington State Department of Ecology.

Fig. 2 The lower Grays River watershed showing A) the model domain, B) the elevation (relative to NAVD88), including the Kandoll Farm site, Seal Slough, Grays River, and Grays Bay, C) patch grid cells (indicated in red) used for calibration of biomass loss based on field measurements between June 2006 and February 2007, D) locations of transects for H-POM flux calculations and the "mask" (black mesh grid) used for the model.

Fig. 3 A) Grays River discharge from Station ID 25B060 for Grays Bay and B) the tidal elevations derived from NOAA Tide Measurements and Predictions.

Fig. 4 Comparisons of measured water-surface elevation and model results at water-level sensor and gage stations. Locations (see Fig. 1b) are A) Channel 1, B) upper Seal Slough inside culverts on Kandoll Farm, C) Reference Channel, and D) Washington State Department of Ecology (WDOE) Grays River flow gage. KF = Kandoll Farm site; GR = Grays River. The vertical datum of the WDOE gage was arbitrary and was adjusted to align with the model during calibration.

Fig. 5 Biomass density and H-POM concentrations throughout the simulation. Biomass density (kg dry mass m^{-2}) A) at the start of the simulation (Hour 1; 15 June 2006); B) prior to the onset of the wet season (Hour 3394; 03 November 2006); and C) at the end of the simulation (Hour 5904; 15 February 2007). H-POM concentration (kg dry mass m^3) D) at the start of the simulation (Hour 1; 15 June 2006); E) prior to the onset of the wet season (Hour 3394; 03 November 2006); and F) at the end of the simulation (Hour 5904; 15 February 2007).

Fig. 6 A) Flow at the three transects where flux calculations were computed (the mouth of the Grays River [Mouth], downstream of the confluence of Seal Slough and Grays River [Confluence], and downstream of the Kandoll Farm (KF) site [Below KF]); B) instantaneous H-POM flux (kg dry mass s^{-1}) at hourly intervals at four transect locations for the entire modeling period, and for the 9-day period illustrating details of the highly variable flux during the peak flood of November 2006 (negative values indicate export of material); and C) cumulative H-POM

mass change at the KF site and the Below KF, Confluence, and Mouth transects. Note that the cumulative mass change at the KF site shows the total H-POM mass mobilized by hydrodynamic forces, measured as kilograms dry weight. See Fig. 2d for locations.

Fig. 7 The flow of H-POM within the site and from the site to the estuary. The percentage values indicate the mass within each box relative to the total peak above-ground biomass density at the Kandoll Farm site.

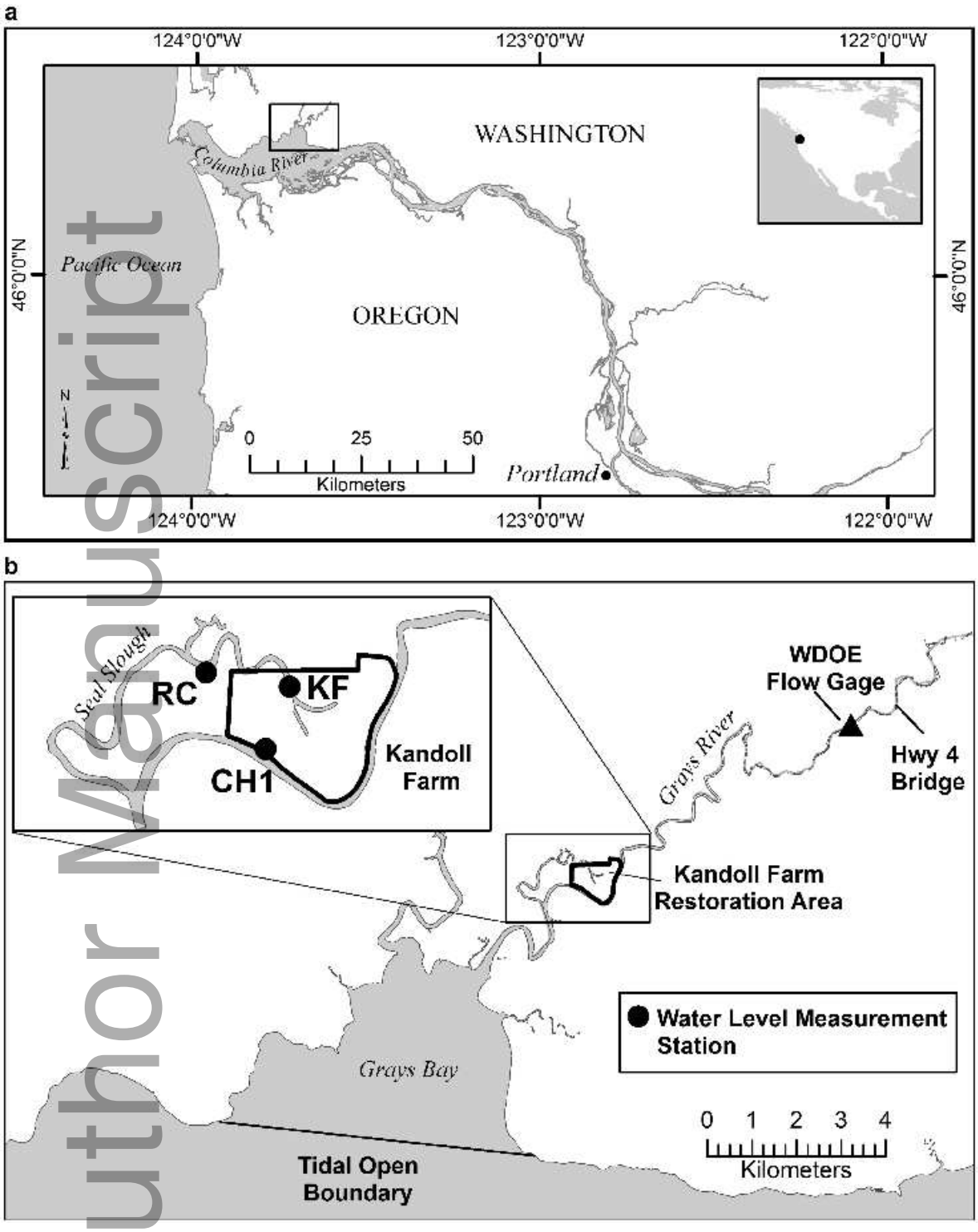

eap_1759_f1.jpg

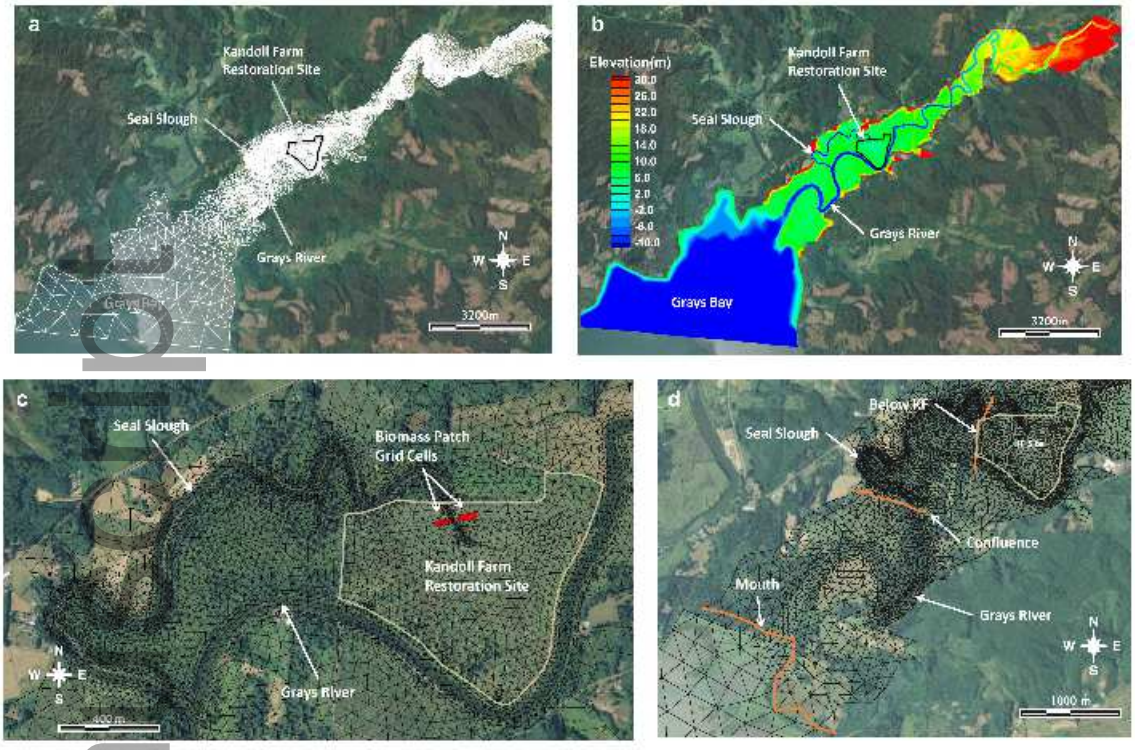

eap_1759_f2.jpg

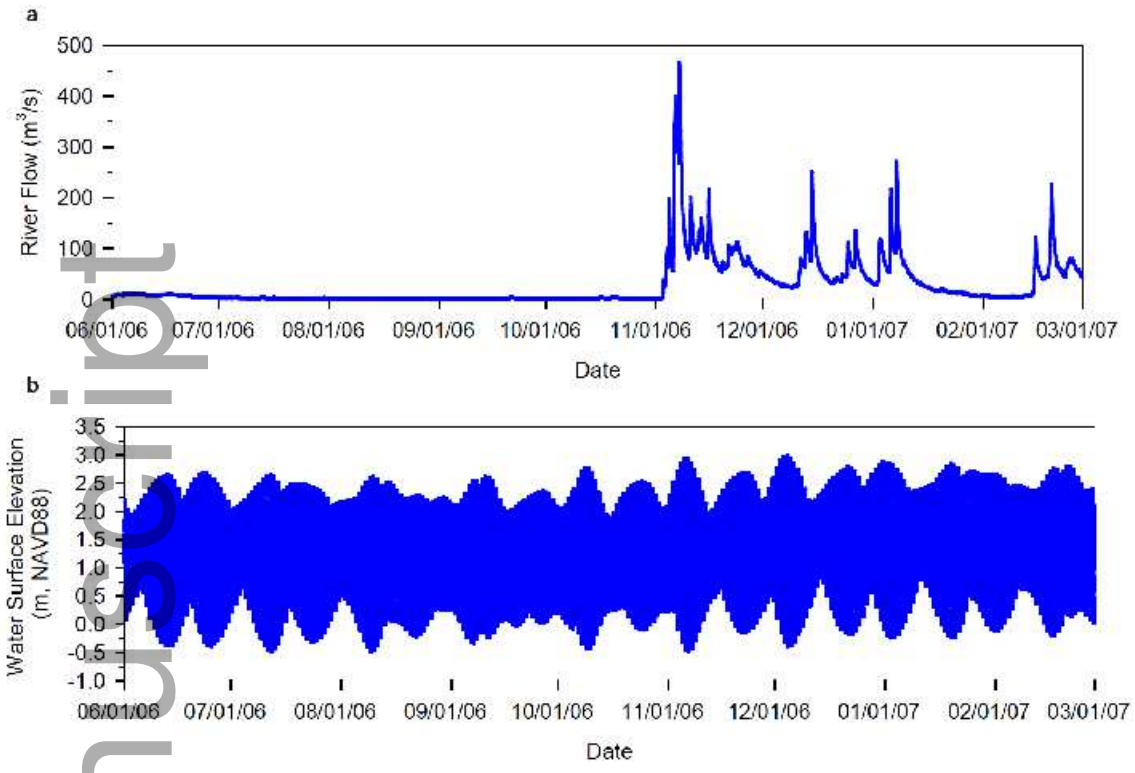

eap_1759_f3.jpg

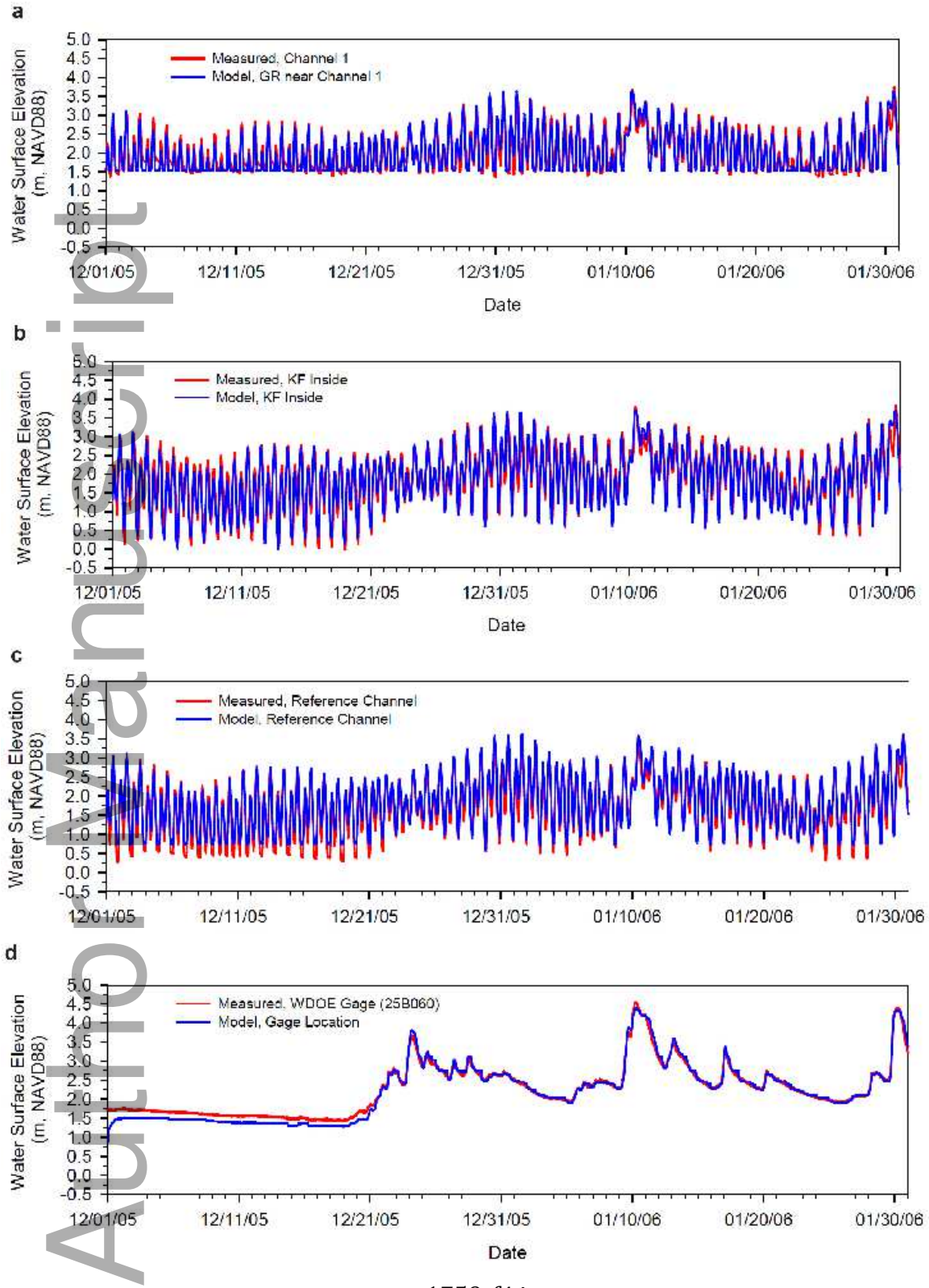

eap_1759_f4.jpg

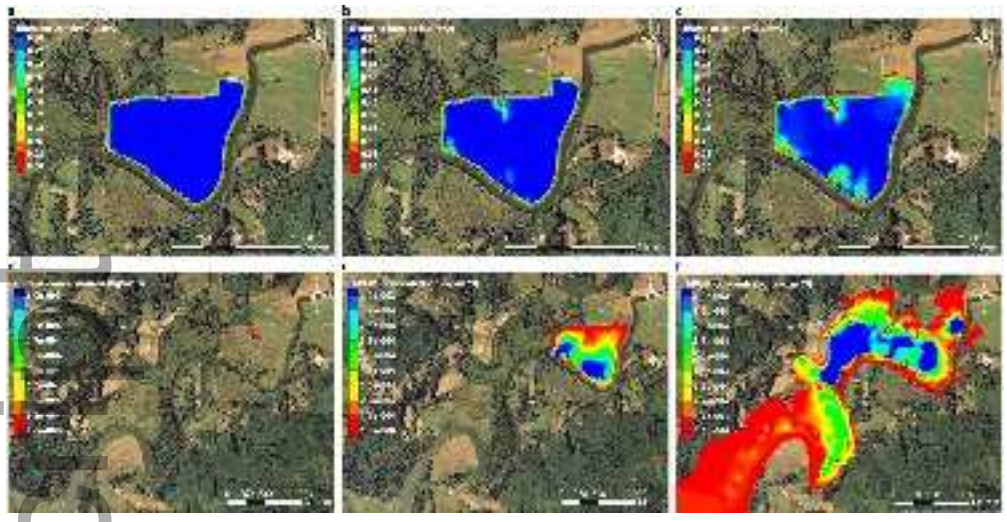

eap_1759_f5.tif

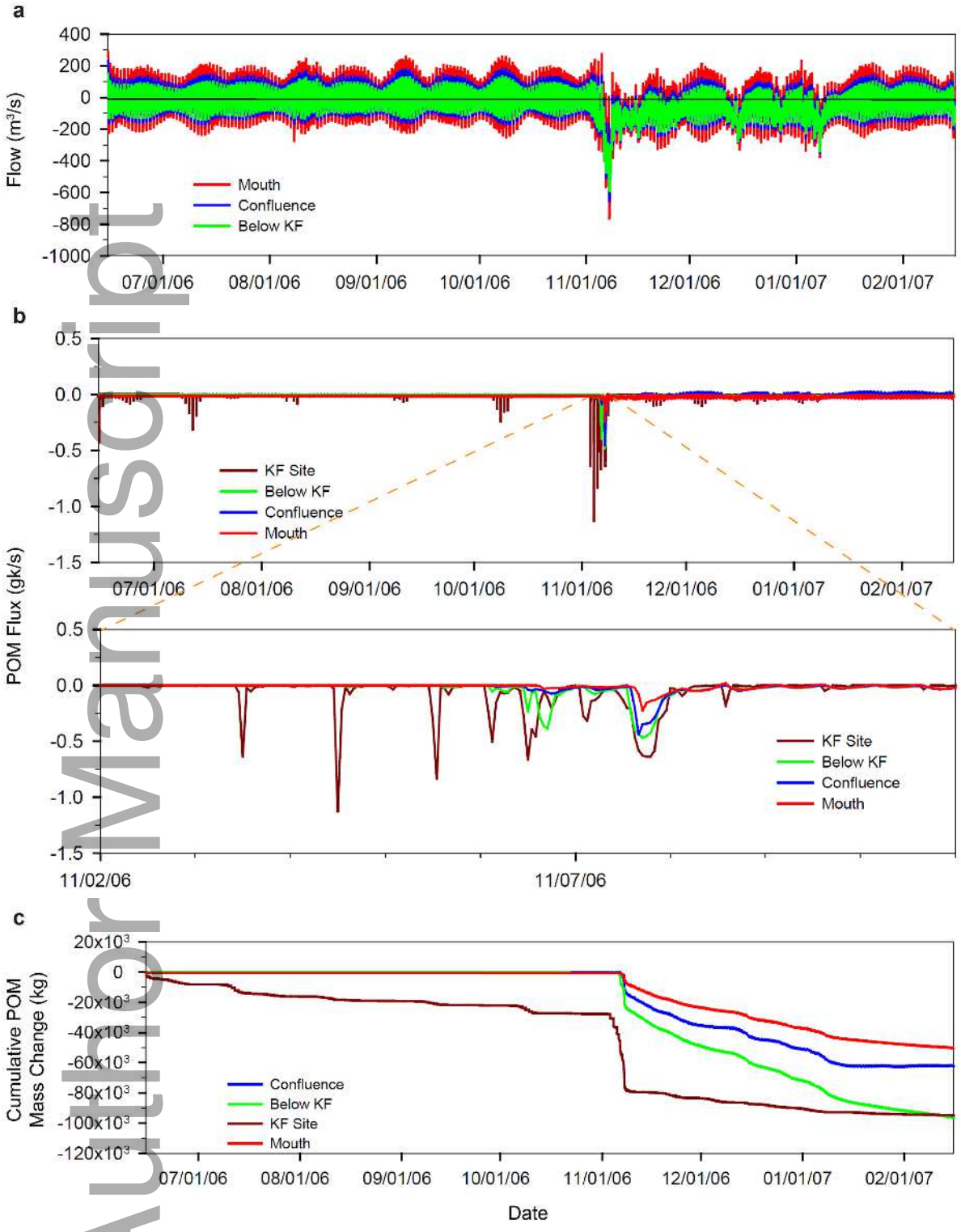

eap_1759_f6.tif

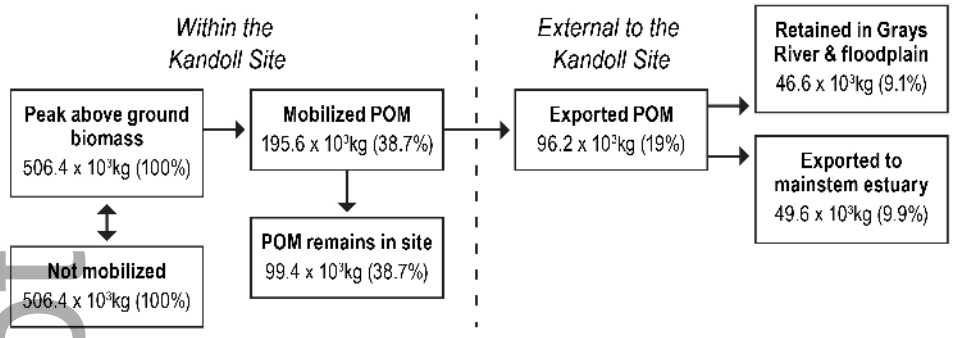

eap_1759_f7.jpg